

Classification between Early Onset Alzheimer's Disease and Frontotemporal Dementia using a single neuroimaging feature

Agnès Pérez-Millan

Alzheimer's Disease and Other Cognitive Disorders Unit, Neurology Service, Hospital Clínic de Barcelona, Institut d'Investigacions Biomèdiques August Pi i Sunyer (IDIBAPS), Fundació Clínic per a la Recerca Biomèdica, Universitat de Barcelona, Barcelona, 08036, Spain.
Institute of Neurosciences. Department of Biomedicine, Faculty of Medicine, University of Barcelona, Barcelona, 08036, Spain.



agperez@recerca.clinic.cat



@agnesperezmi



SPIE. OPTICS + PHOTONICS

INTRODUCTION: Early Onset Dementia

- ❖ Early-onset dementia = dementia with onset under age 65.

INTRODUCTION: Early Onset Dementia

- ❖ Early-onset dementia = dementia with onset under age 65.
- ❖ Early Onset Alzheimer's Disease (EOAD) and Frontotemporal Dementia (FTD) are common forms of early-onset dementia.

INTRODUCTION: Early Onset Dementia

- ❖ Early-onset dementia = dementia with onset under age 65.
- ❖ Early Onset Alzheimer's Disease (EOAD) and Frontotemporal Dementia (FTD) are common forms of early-onset dementia.
- ❖ Alzheimer's Disease (AD) is characterized by progressive memory loss accompanied with language, executive and visuospatial problems.

INTRODUCTION: Early Onset Dementia

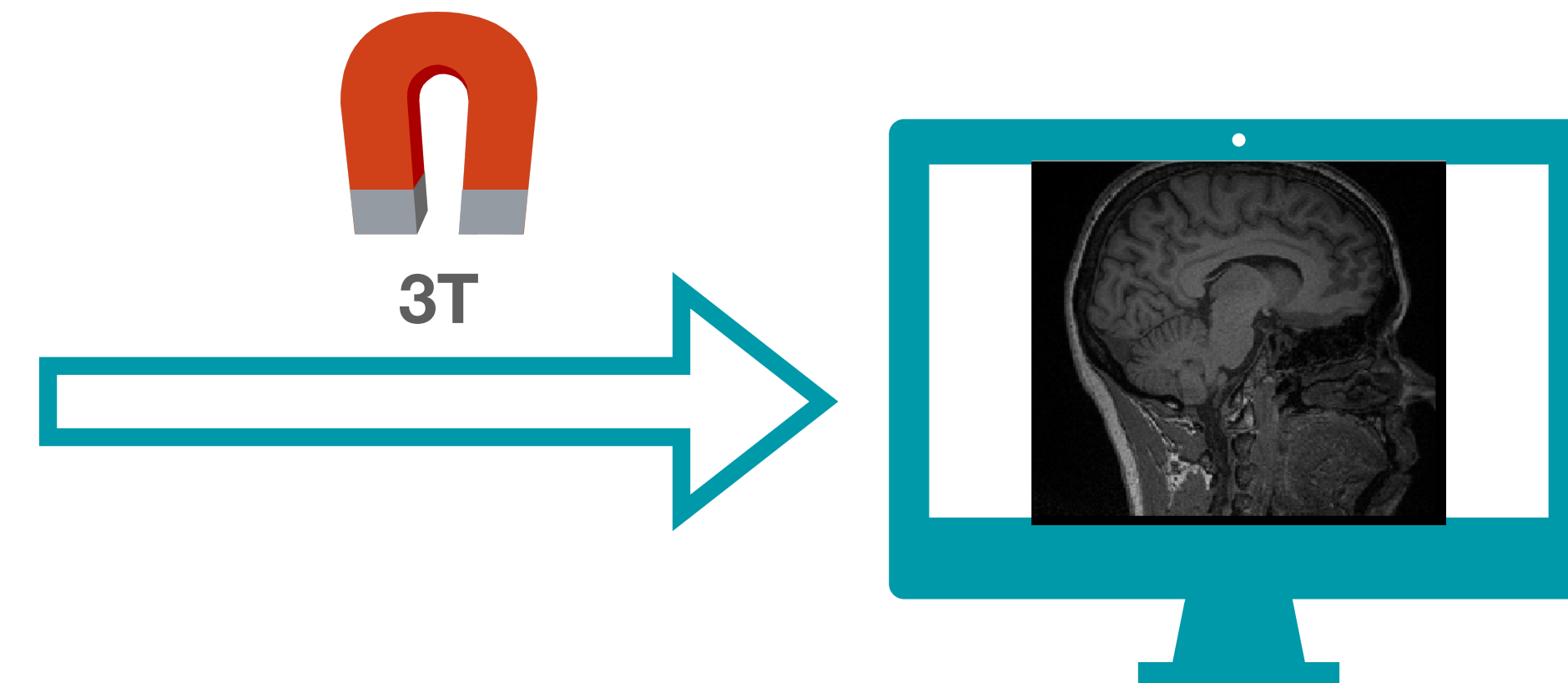
- ❖ Early-onset dementia = dementia with onset under age 65.
- ❖ Early Onset Alzheimer's Disease (EOAD) and Frontotemporal Dementia (FTD) are common forms of early-onset dementia.
- ❖ Alzheimer's Disease (AD) is characterized by progressive memory loss accompanied with language, executive and visuospatial problems.
- ❖ FTD is characterized by progressive behavioural, executive and language problems.

INTRODUCTION: Challenging Diagnosis

- ❖ In the clinical practice the overlapping symptoms and brain signatures makes the diagnosis challenging.

INTRODUCTION: Challenging Diagnosis

- ❖ In the clinical practice the overlapping symptoms and brain signatures makes the diagnosis challenging.
- ❖ Magnetic Resonance Imaging (MRI) has been widely used to detect disease-specific brain changes across these disorders.



INTRODUCTION: Challenging Diagnosis

- ❖ In the clinical practice the overlapping symptoms and brain signatures makes the diagnosis challenging.
- ❖ Magnetic Resonance Imaging (MRI) has been widely used to detect disease-specific brain changes across these disorders.
- ❖ Distinct brain atrophy patterns could potentially help in differentiating EOAD and FTD.

INTRODUCTION: Challenging Diagnosis

- ❖ In the clinical practice the overlapping symptoms and brain signatures makes the diagnosis challenging.
- ❖ Magnetic Resonance Imaging (MRI) has been widely used to detect disease-specific brain changes across these disorders.
- ❖ Distinct brain atrophy patterns could potentially help in differentiating EOAD and FTD.
- ❖ Unsupervised and supervised machine learning were combined to discriminate between EOAD, FTD and healthy controls (CTR).

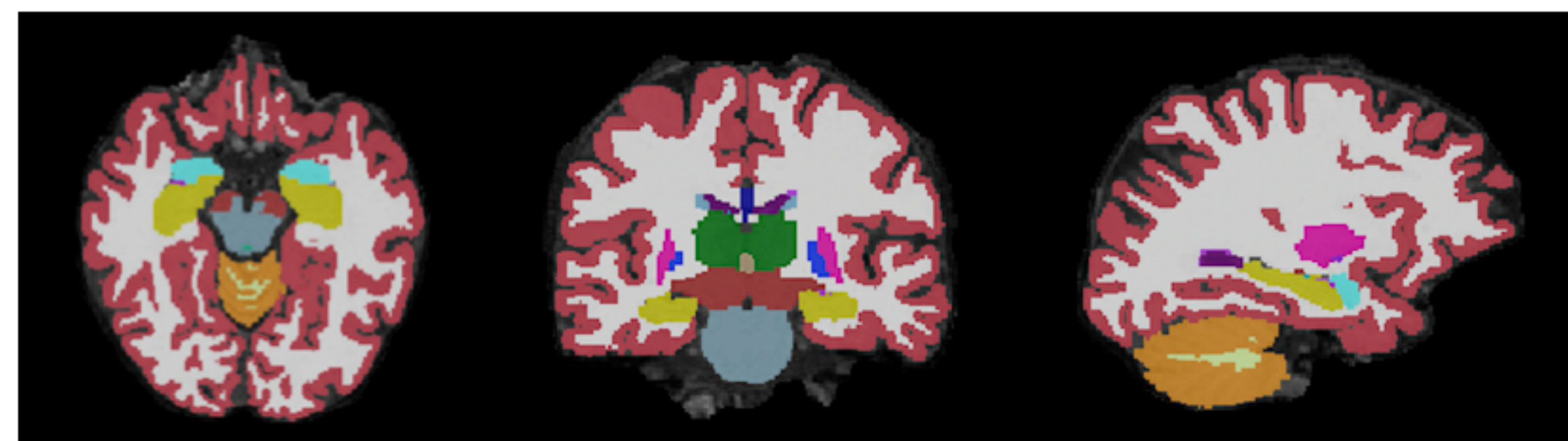
AIM

**To develop a classification algorithm using MRI data including EOAD and FTD,
while providing interpretability of the results.**

SAMPLE DEMOGRAPHICS

Table 1. Group summaries given as the mean and the standard deviation of each measure. Differences between groups are calculated using Fisher exact Test for sex and ANOVA test for age at MRI.

	CTR	EOAD	FTD	CTR-EOAD p-value	CTR-FTD p-value	EOAD-FTD p-value
Number of participants	66	85	52	—	—	—
Sex (Men/Women)	18/48	35/50	30/22	0.087	0.0038	0.087
Age at MRI, years (SD)	54.95 (8.40)	57.29 (6.13)	57.89 (4.85)	0.052	0.052	0.061

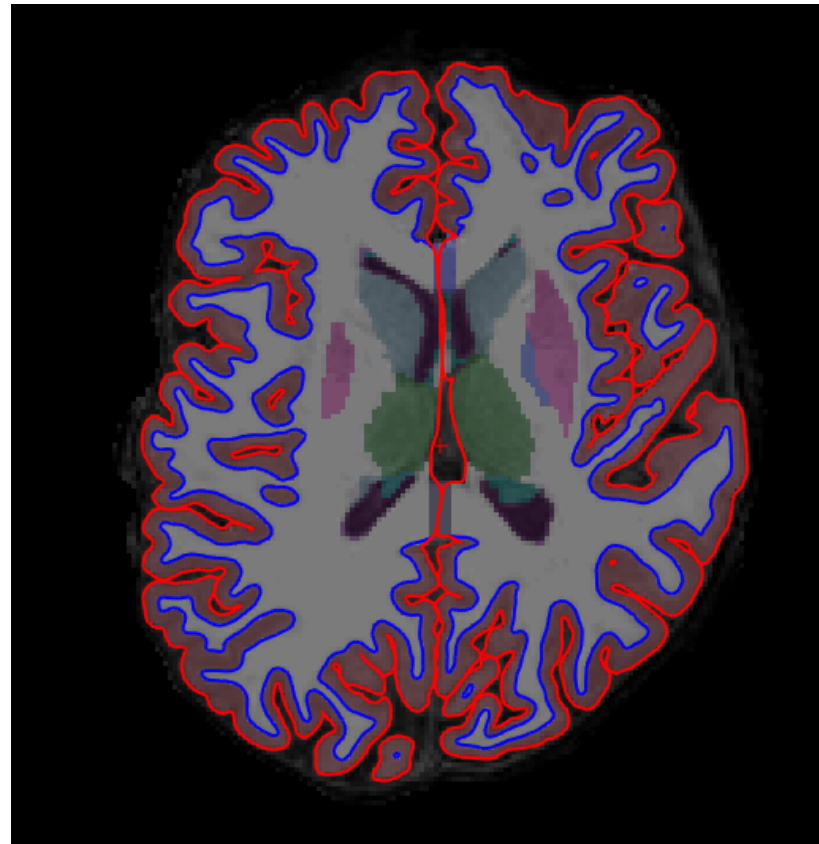


ALGORITHM



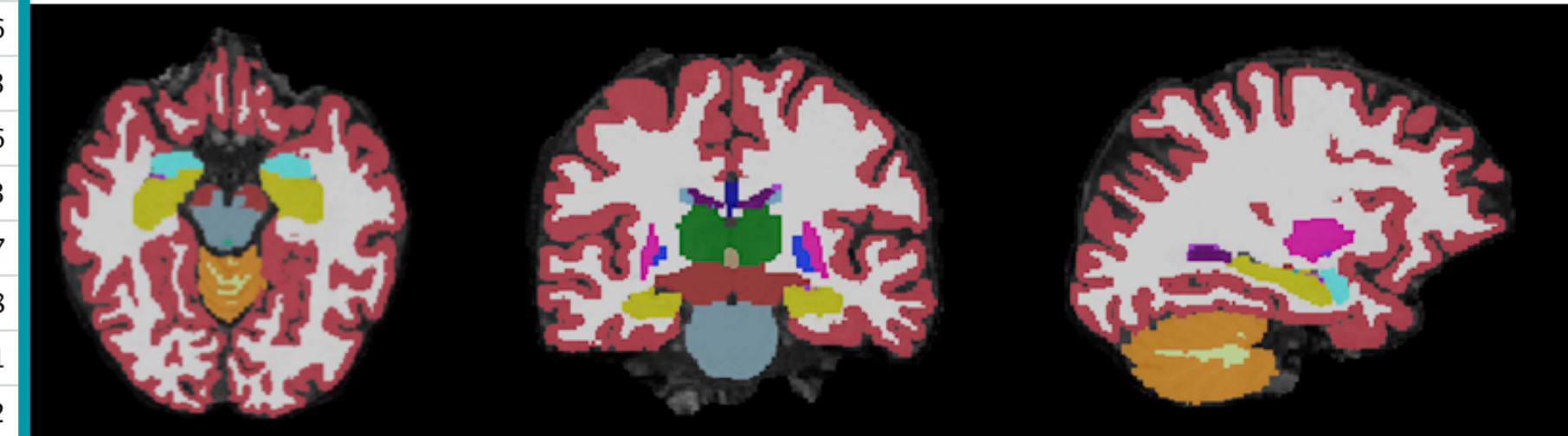
FreeSurfer

INPUT:
Subcortical gray
matter volumes and
cortical thickness



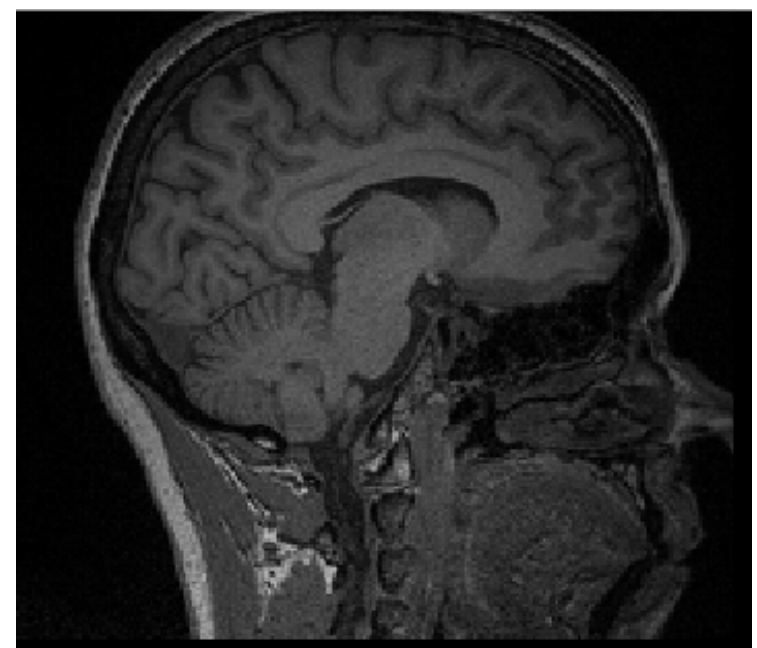
rh_caudalanteriorcingulate_thickness	rh_caudalmiddlefrontal_thickness	rh_cuneus_thickness	rh_entorhinal_thickness	rh_fusiform_thickness
2.523	2.474	1.824	3.608	2.722
2.245	2.417	1.897	3.093	2.788
2.782	2.296	2.043	4.120	2.738
2.222	2.029	2.057	3.581	2.754
2.451	2.230	1.876	2.692	2.339
2.235	2.421	1.900	3.391	2.847
2.332	2.346	1.762	2.890	2.604
2.534	2.383	1.767	3.202	2.308
2.744	2.315	1.943	3.416	2.457
2.398	2.181	1.960	3.853	2.565
2.396	2.310	1.944	3.363	2.921
2.386	2.344	1.809	3.340	2.666
2.516	2.339	1.498	3.455	2.391
2.342	2.350	1.823	3.215	2.617
2.731	2.121	1.815	3.186	2.471
2.773	2.482	1.775	3.192	2.790
2.235	2.132	1.933	2.343	2.147
2.652	2.157	1.919	3.170	2.799
2.280	2.464	2.078	2.987	2.753
2.027	2.266	1.932	3.274	2.374

Left.Thalamus.Proper	Left.Caudate	Left.Putamen	Left.Pallidum
6048.0	3038.4	3935.0	1710.0
7435.4	3268.5	4772.1	2105.6
5559.7	2087.7	3661.5	1429.3
6396.7	2756.8	4411.9	1909.6
5126.6	2344.7	3169.7	1729.3
7240.5	2889.3	3333.4	1805.7
7143.6	3296.8	4073.7	1897.8
7364.9	3430.2	4414.5	2030.1
6240.1	3553.8	3877.7	1819.2
7290.9	3187.6	4667.2	2215.5
7533.0	3141.6	4452.9	2283.9



We used FreeSurfer to obtain subcortical gray matter volumes and cortical thickness from T1w MRI images to train our algorithm.

ALGORITHM



FreeSurfer

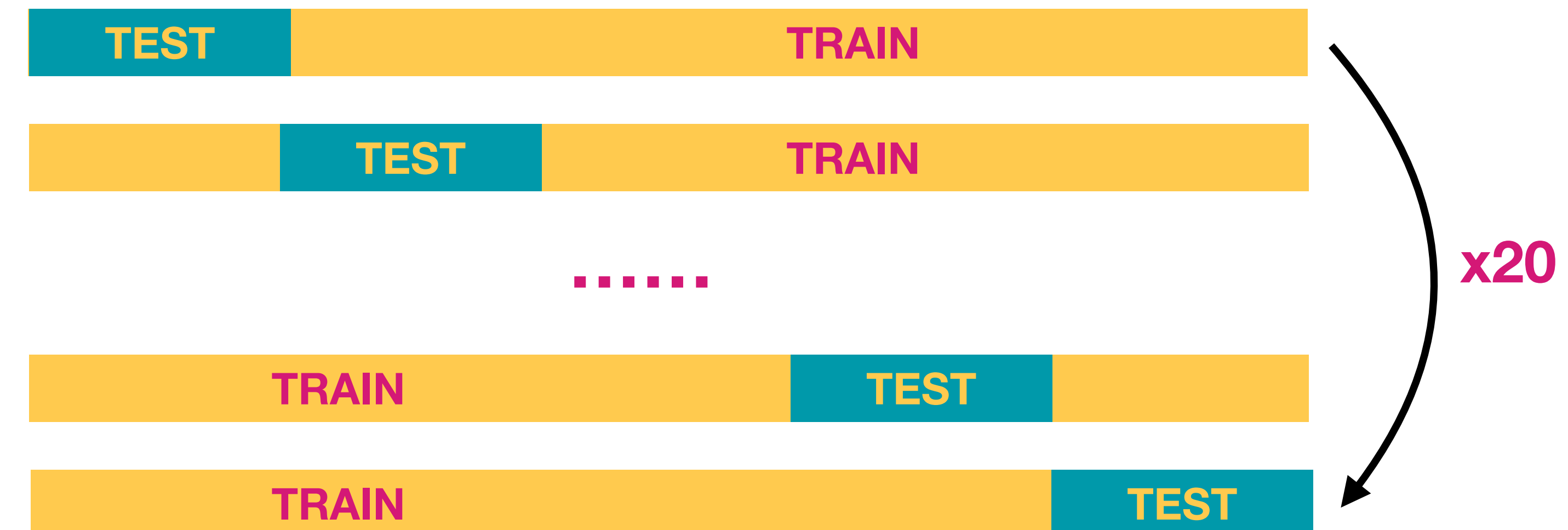
INPUT:
Subcortical gray
matter volumes and
cortical thickness

TRAIN SET

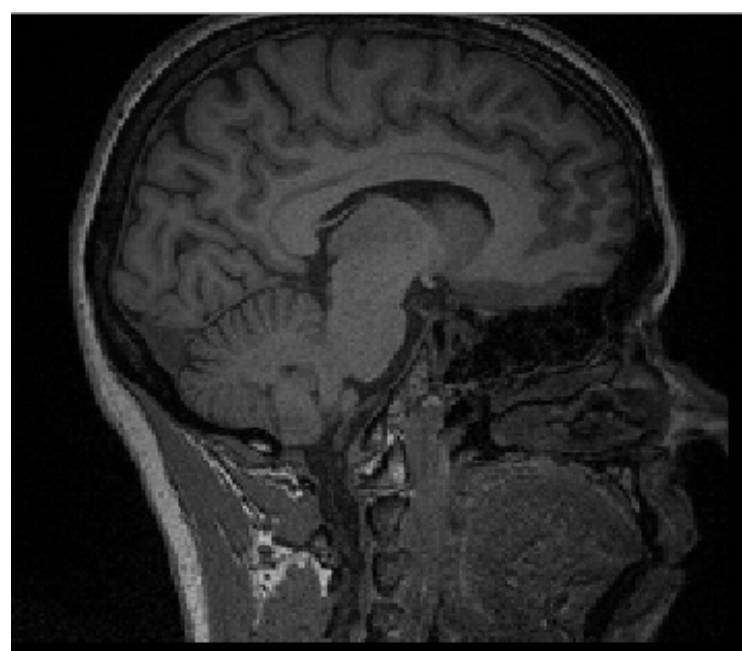
TEST SET

k-fold
cross-
validation

We splitted the data into train and test datasets with a k-fold cross-validation.

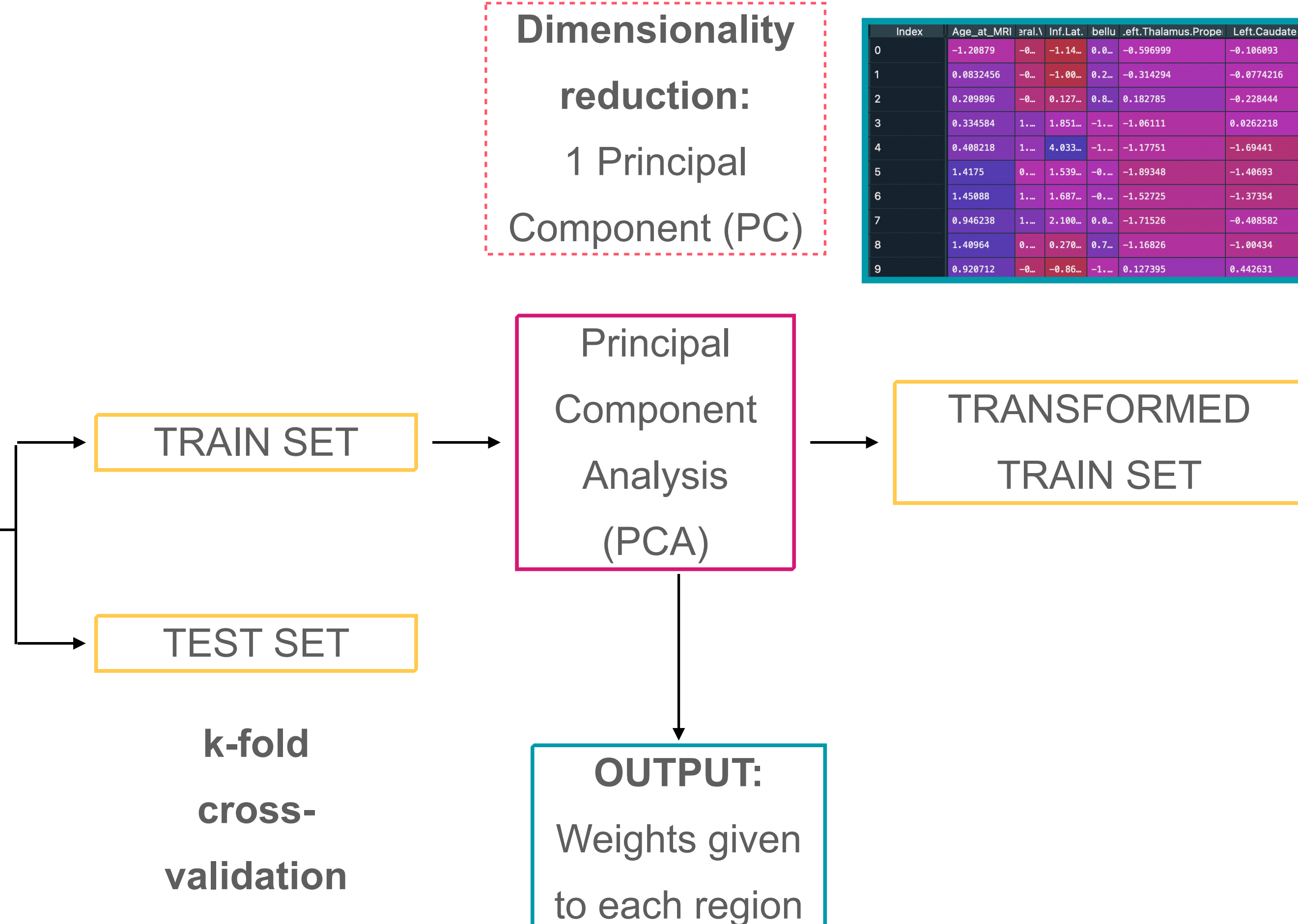


ALGORITHM



FreeSurfer

INPUT:
Subcortical gray
matter volumes and
cortical thickness

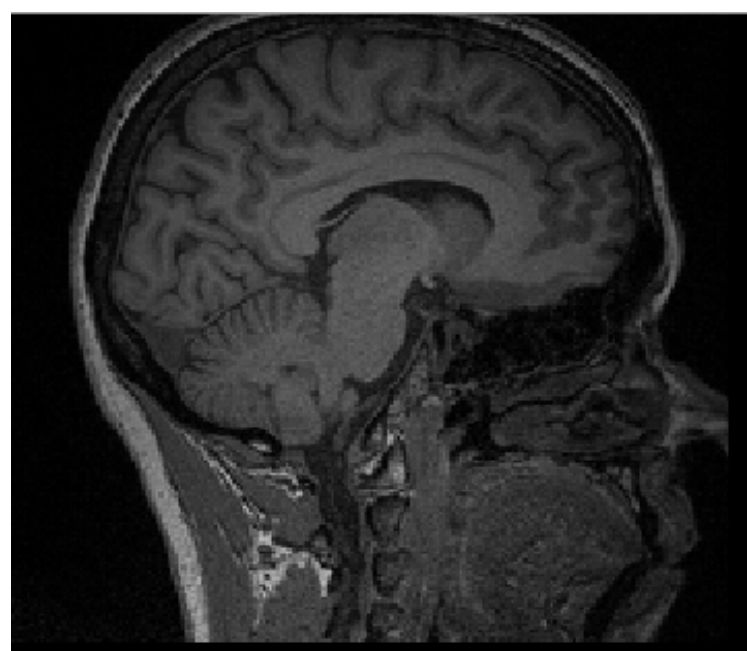


Index	Age_at_MRI	lateral.V	Inf.Lat.	bellu	Left.Thalamus.Prope	Left.Caudate	Left.Putamen	Left.Pallidum	Left.Hippocampus	Left.Amygdala	cumbe	roid	astral.V	.Inf.Lat	ebellu	Right.Thalamus.Propel	Right.Caudate
0	-1.20879	-0...	-1.14...	0.0...	-0.596999	-0.106093	-0.282156	-0.793601	0.241611	1.00379	0.75...	-1...	-0.71...	-0.9...	-0.1...	-1.04795	-0.311487
1	0.0832456	-0...	-1.00...	0.2...	-0.314294	-0.0774216	-0.213605	-0.585758	-0.263446	-0.209823	0.21...	-0...	-0.02...	-0.9...	-0.1...	-1.38358	-0.33936
2	0.209996	-0...	0.127...	0.8...	0.182785	-0.228444	-0.203529	0.487253	-0.997618	-1.52422	-0.2...	-0...	-0.57...	-0.1...	1.26...	0.173688	-0.0049531
3	0.334584	1...	1.851...	-1...	-1.06111	0.0262218	-0.498637	-0.631365	-1.3831	-1.72891	-1.4...	0.0...	1.457...	-0.1...	-1.0...	-0.599923	0.563366
4	0.408218	1...	4.033...	-1...	-1.17751	-1.69441	-2.24398	-1.54868	-2.19693	-1.38496	-0.4...	-0...	2.447...	4.86...	-1.5...	-2.04065	-1.54436
5	1.4175	0...	1.539...	-0...	-1.89348	-1.40693	-1.52225	-0.243069	-0.534128	-1.36953	-1.8...	-0...	0.662...	1.02...	-1.4...	-1.61707	-0.747341
6	1.45088	1...	1.687...	-0...	-1.52725	-1.37354	-1.61841	-1.72411	-2.25535	-2.03689	-0.6...	1.1...	2.181...	2.90...	-0.4...	-1.68142	-0.668878
7	0.946238	1...	2.100...	0.0...	-1.71526	-0.408582	-1.38296	1.27475	-0.844835	-1.36974	-0.6...	1.8...	1.096...	0.73...	0.49...	-0.805792	-0.621221
8	1.40964	0...	0.270...	0.7...	-1.16826	-1.00434	-0.375499	-0.569332	-1.0279	0.157696	-1.6...	0.7...	-0.06...	0.00...	0.04...	-2.17336	-0.602281
9	0.920712	-0...	-0.86...	-1...	0.127395	0.442631	0.245403	0.441244	-1.6176	-0.958503	-0.0...	-1...	-0.27...	-0.8...	-0.6...	0.32038	1.06763

Index	0
0	-0.180822
1	0.0626757
2	0.124022
3	0.110981
4	0.691609
5	0.467265
6	0.851905
7	0.426191
8	0.254307
9	-0.177468
10	0.192423
11	0.263028
12	-0.0625034
13	0.179495
14	-0.167746
15	0.475608

We applied a dimensionality reduction using PCA. We only kept the first PC. We obtained the transformed dataset and the weights of all the features which give us the first PC.

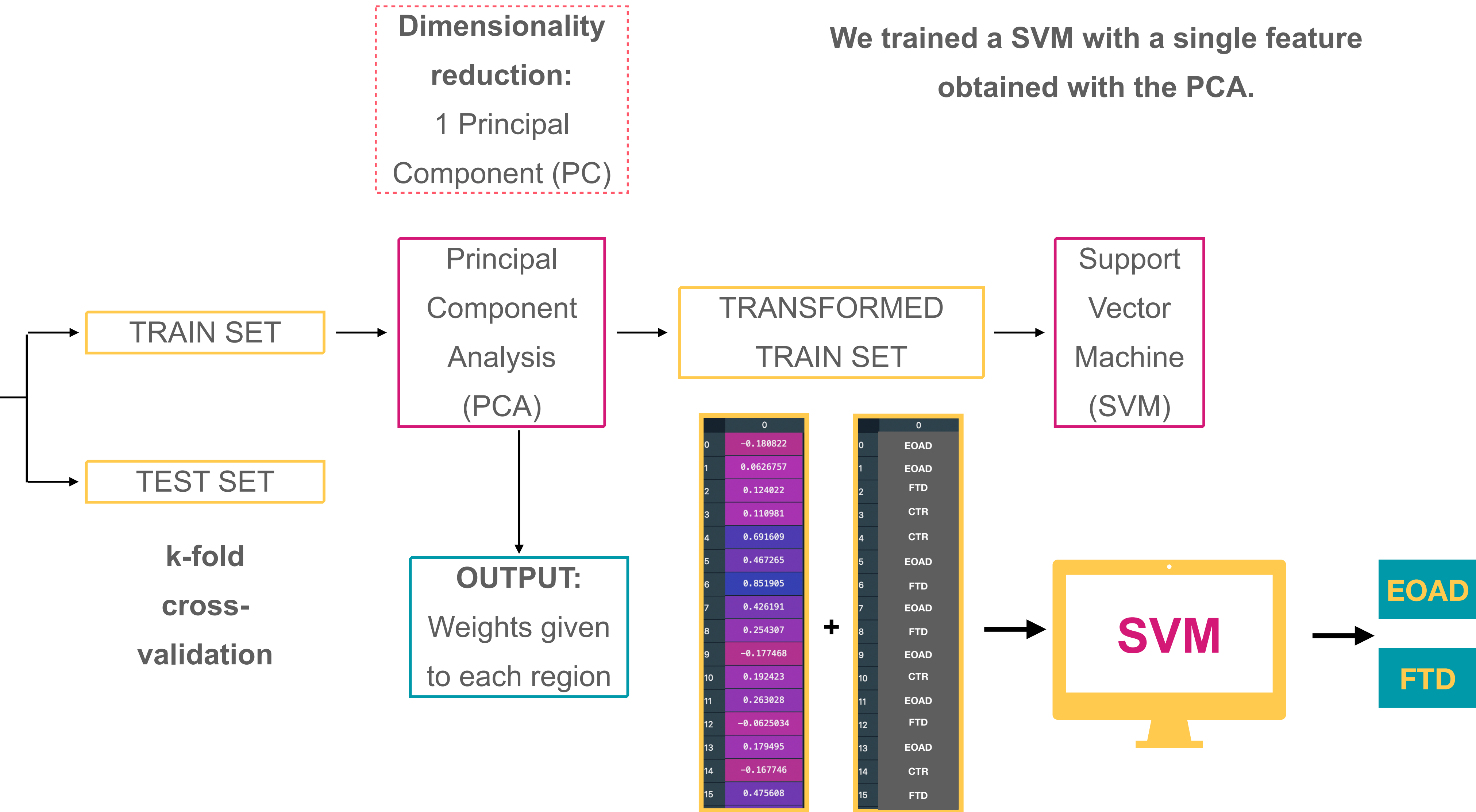
ALGORITHM



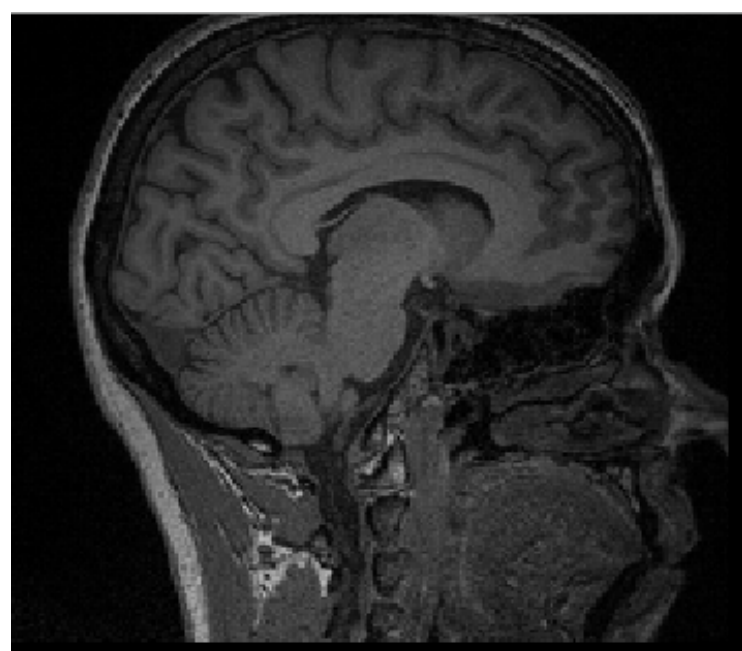
FreeSurfer

INPUT:
Subcortical gray
matter volumes and
cortical thickness

k-fold
cross-
validation



ALGORITHM

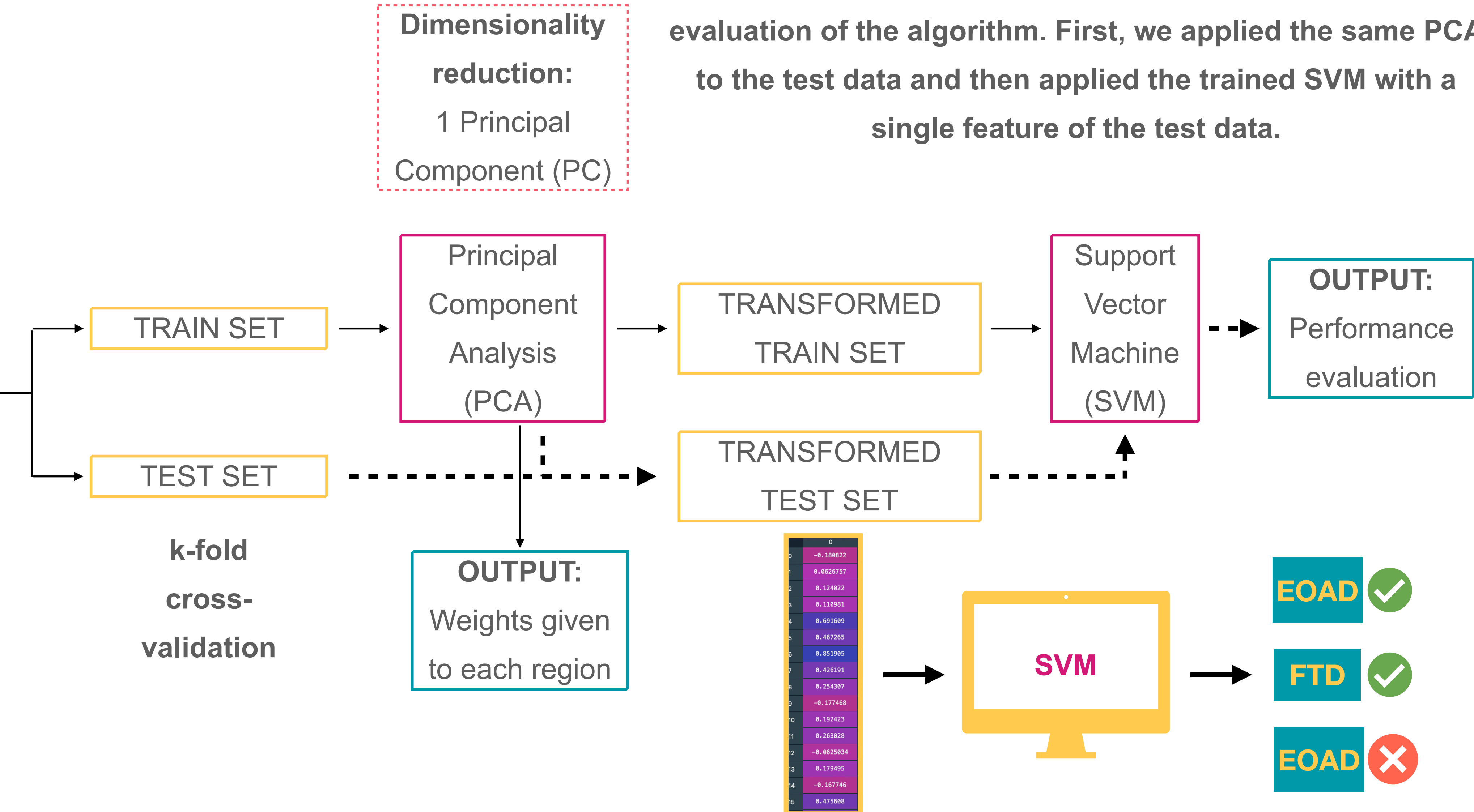


FreeSurfer

INPUT:

Subcortical gray matter volumes and cortical thickness

k-fold cross-validation



RESULTS: Classification

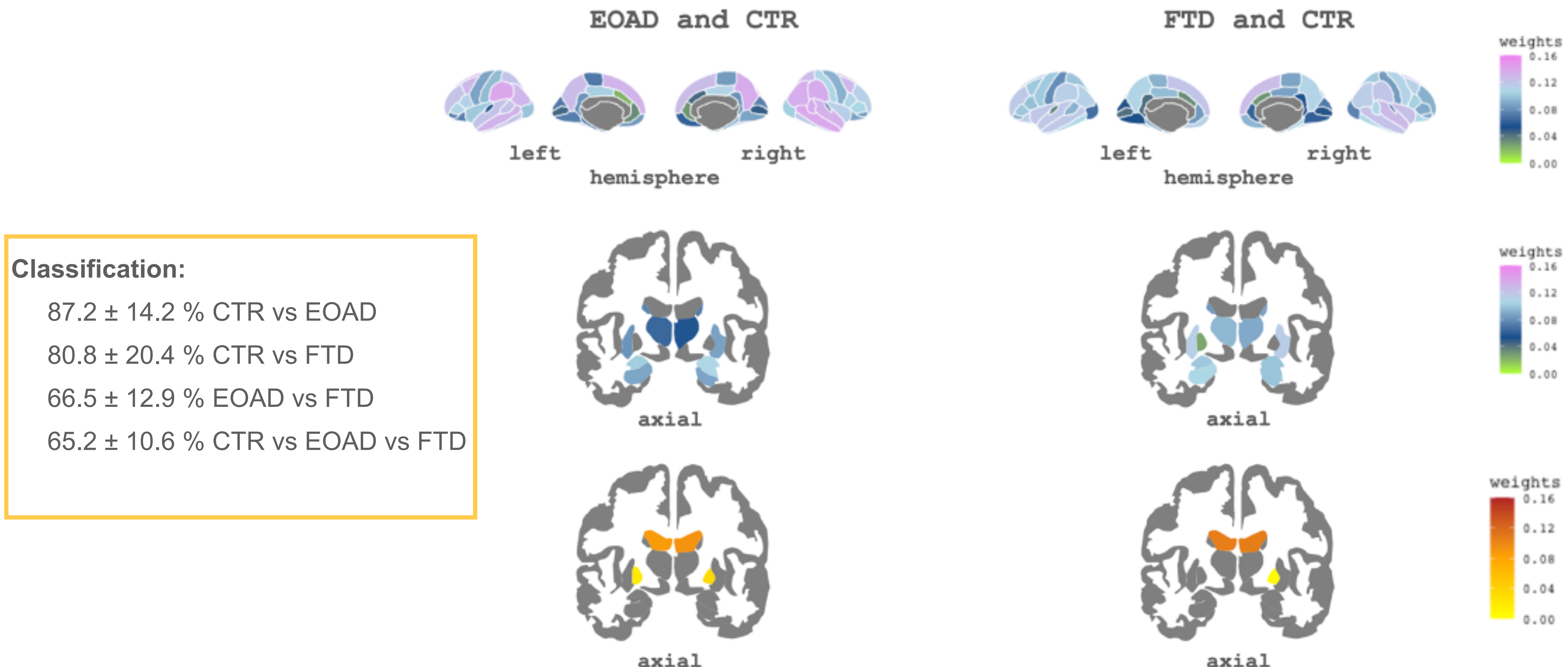


Figure 1. Subcortical and cortical patterns of the first PC's weights associated with EOAD and FTD. Top: Cortical ROIs included in the component. Bottom: subcortical ROIs of the component. Cool color scale represents negative weights and warm scale represents positive weights within the component.

RESULTS: Patterns

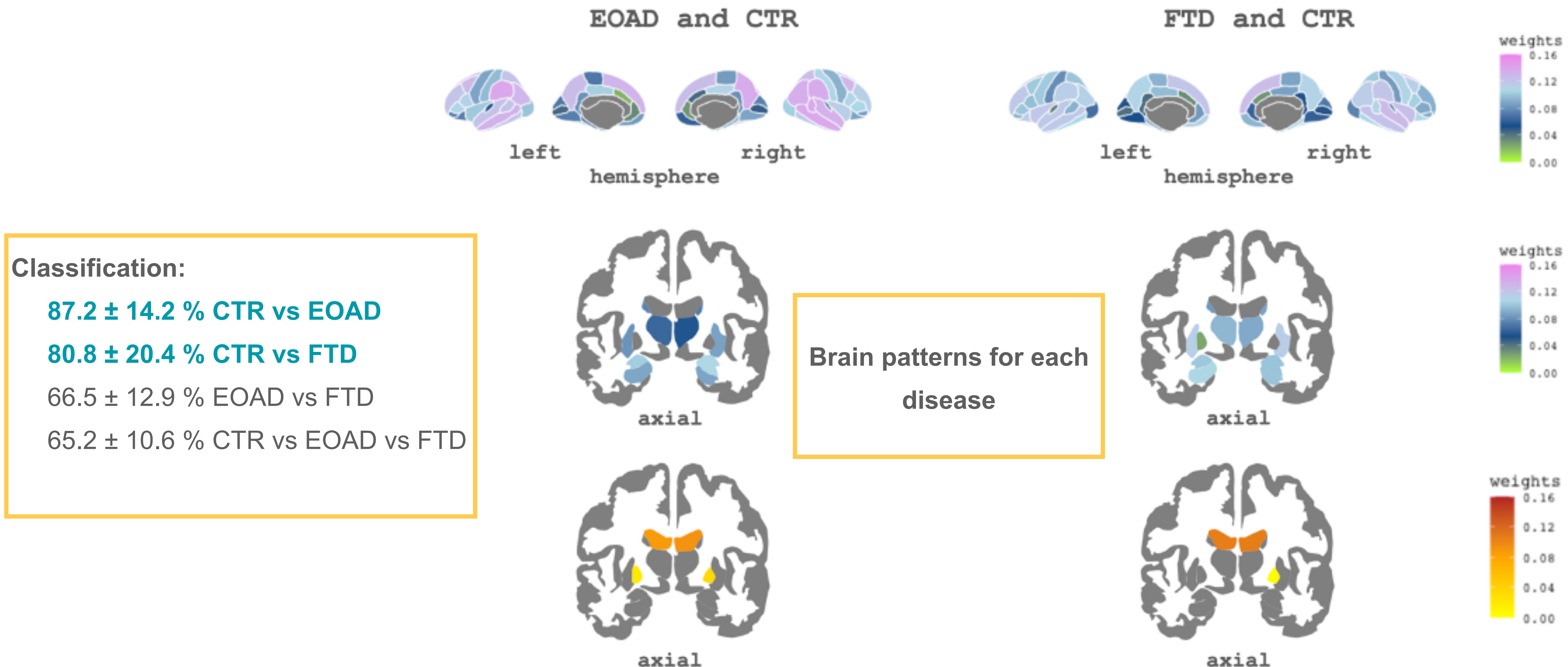


Figure 1. Subcortical and cortical patterns of the first PC's weights associated with EOAD and FTD. Top: Cortical ROIs included in the component. Bottom: subcortical ROIs of the component. Cool color scale represents negative weights and warm scale represents positive weights within the component.

DISCUSSION: Classification

Classification:

$87.2 \pm 14.2\%$ CTR vs EOAD

$80.8 \pm 20.4\%$ CTR vs FTD

$66.5 \pm 12.9\%$ EOAD vs FTD

$65.2 \pm 10.6\%$ CTR vs EOAD vs FTD

Published Papers^{1,2,3,4}:

80-95 % CTR vs EOAD (or AD)

72-88 % CTR vs FTD

69-89 % EOAD (or AD) vs FTD

70 % CTR vs AD vs FTD

REFERENCES:

- [1] Möller, C., Pijnenburg, Y. A. L., Van Der Flier, W. M., Versteeg, A., Tijms, B., De Munck, J. C., Hafkemeijer, A., Rombouts, S. A. R. B., Van Der Grond, J., Van Swieten, J., Dopper, E., Scheltens, P., Barkhof, F., Vrenken, H. and Wink, A. M., "Alzheimer disease and behavioral variant frontotemporal dementia: Automatic classification based on cortical atrophy for single-subject diagnosis," *Radiology* 279(3), 838-848 (2016).
- [2] Bron, E. E., Smits, M., Papma, J. M., Steketee, R. M. E., Meijboom, R., de Groot, M., van Swieten, J. C., Niessen, W. J. and Klein, S., "Multiparametric computer-aided differential diagnosis of Alzheimer's disease and frontotemporal dementia using structural and advanced MRI," *Eur. Radiol.* 27(8), 3372-3382 (2017).
- [3] Klöppel, S., Stonnington, C. M., Chu, C., Draganski, B., Scahill, R. I., Rohrer, J. D., Fox, N. C., Jack, C. R., Ashburner, J. and Frackowiak, R. S. J., "Automatic classification of MR scans in Alzheimer's disease," *Brain* 131(3), 681-689 (2008).
- [4] Chagué, P., Marro, B., Fadili, S., Houot, M., Morin, A., Samper-González, J., Beunon, P., Arrivé, L., Dormont, D., Dubois, B., Teichmann, M., Epelbaum, S. and Colliot, O., "Radiological classification of dementia from anatomical MRI assisted by machine learning-derived maps," *J. Neuroradiol.* 48(6), 412-418 (2021).

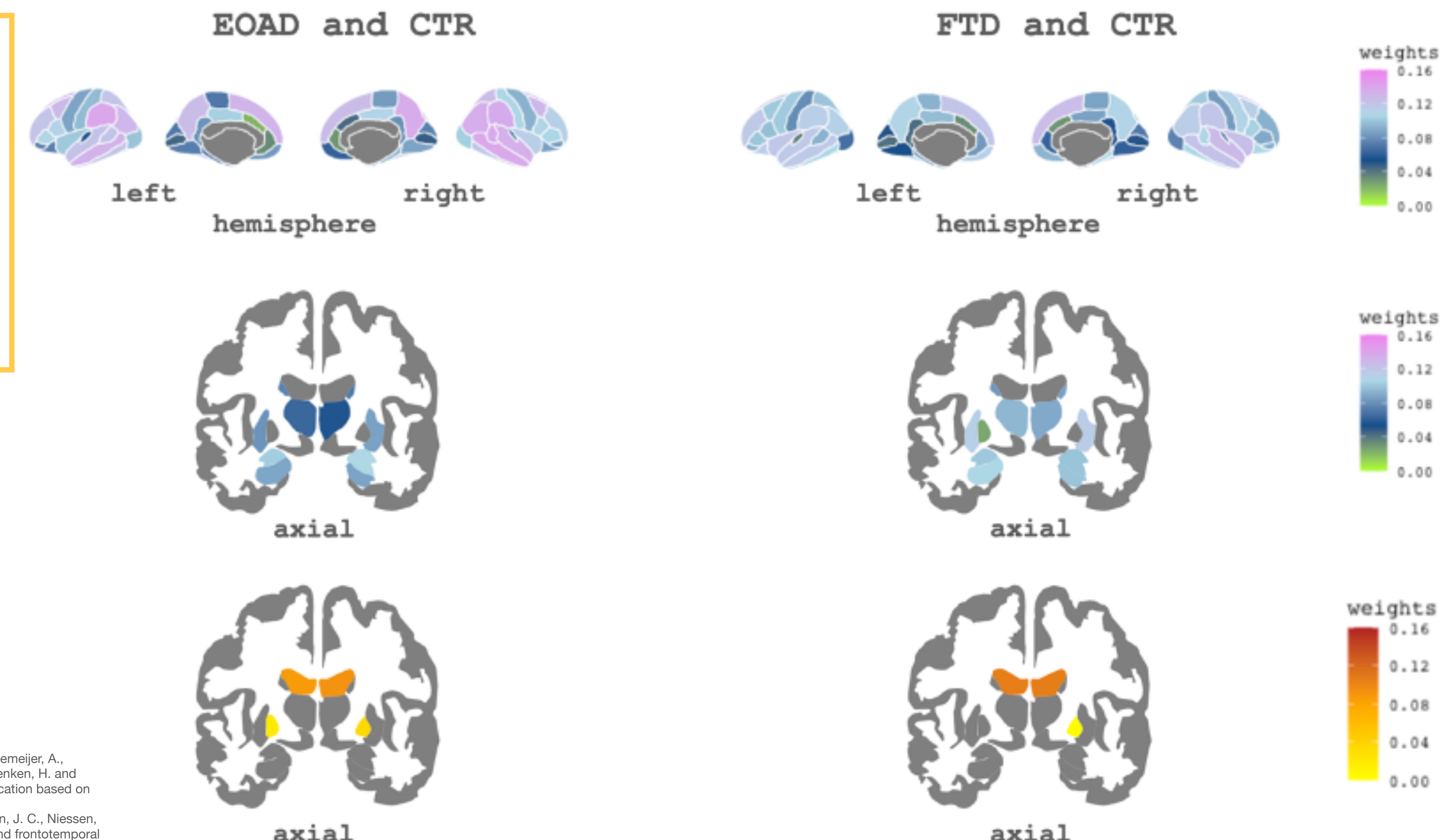


Figure 1. Subcortical and cortical patterns of the first PC's weights associated with EOAD and FTD. Top: Cortical ROIs included in the component. Bottom: subcortical ROIs of the component. Cool color scale represents negative weights and warm scale represents positive weights within the component.

DISCUSSION: Patterns

Classification:

$87.2 \pm 14.2\% \text{ CTR vs EOAD}$

$80.8 \pm 20.4\% \text{ CTR vs FTD}$

$66.5 \pm 12.9\% \text{ EOAD vs FTD}$

$65.2 \pm 10.6\% \text{ CTR vs EOAD vs FTD}$

Brain patterns for each disease



Interpretability of the results

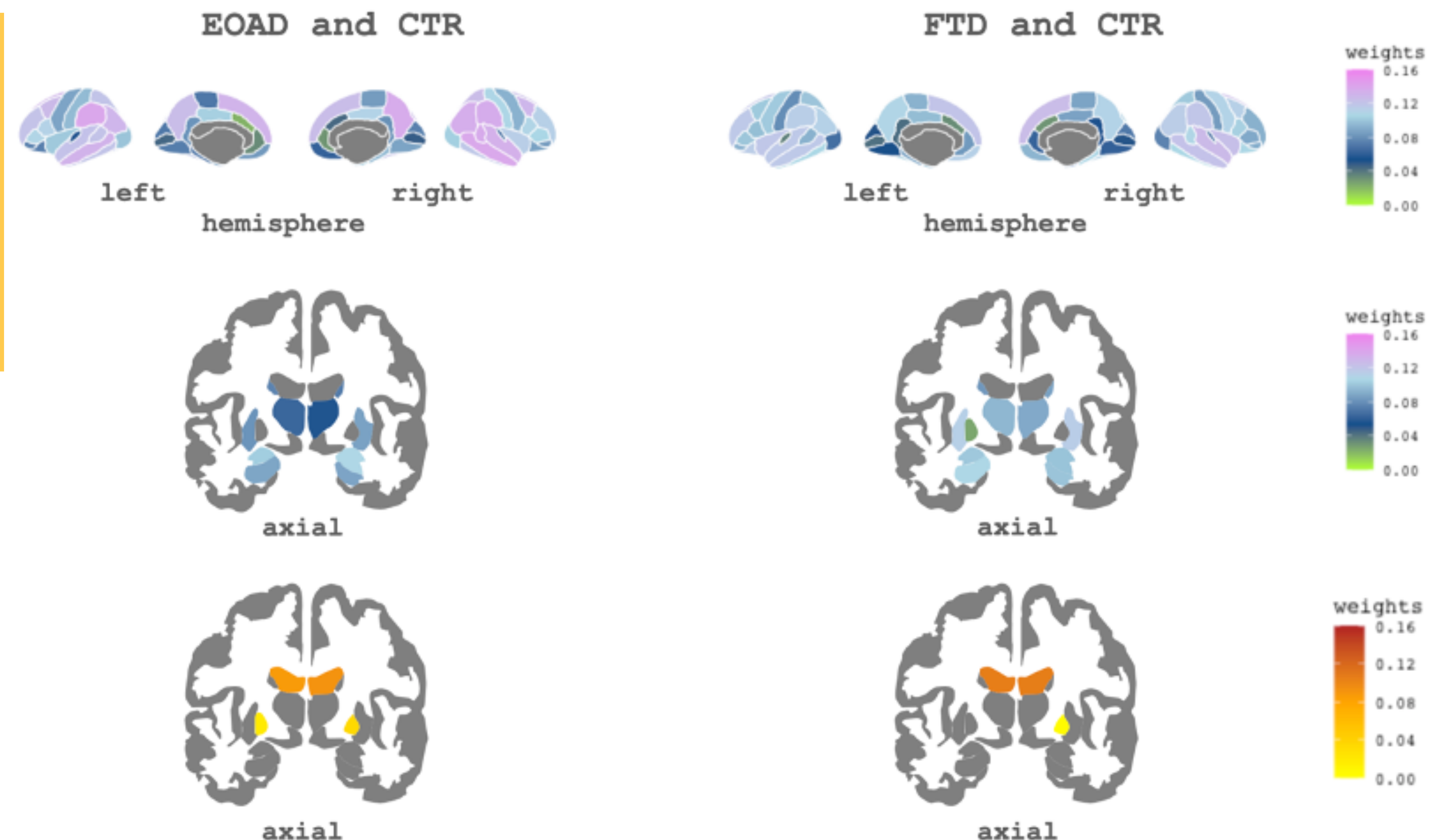


Figure 1. Subcortical and cortical patterns of the first PC's weights associated with EOAD and FTD. Top: Cortical ROIs included in the component. Bottom: subcortical ROIs of the component. Cool color scale represents negative weights and warm scale represents positive weights within the component.

CONCLUSIONS

The combination of unsupervised and supervised techniques of machine learning provided the opportunity of:

1. Reducing all subcortical gray matter volumes and cortical thickness measures into a single feature.
2. Obtaining good accuracy classifying EOAD, FTD and CTR.
3. Giving interpretability of the results with the atrophy patterns.

Thanks!

José Contador, Mircea Balasa, Albert Lladó &
Raquel Sánchez-Valle



Laia Borrell & Roser Sala-Llonch



agperez@recerca.clinic.cat

[@agnesperezmi](https://twitter.com/agnesperezmi)

CLÍNIC
BARCELONA
Hospital Universitari

IDIBAPS

Institut
D'Investigacions
Biomèdiques
August Pi i Sunyer

UNIVERSITAT DE
BARCELONA

Facultat de Medicina
i Ciències de la Salut



Institut de Neurociències
UNIVERSITAT DE BARCELONA

Institut de Salud Carlos III
Ministerio de Ciencia e Innovación
Unión Europea
Fondo Europeo de Desarrollo Regional
"Una manera de hacer Europa"

Generalitat de Catalunya
Departament de Salut

ACKNOWLEDGEMENTS: The authors thank patients, their relatives, and healthy controls for their participation in the research. A. Pérez-Millan is a recipient of the Optics + Photonics Student Conference Support from the SPIE Student Conference Support and Conference Travel fellowship from the University of Barcelona. This work was supported by Instituto de Salud Carlos III, Spain (grant no. 20143810 and PI20/0448 to Dr. R. Sanchez-Valle), Spanish Ministry of Science and by Instituto de Salud Carlos III (ISCIII) and co-funded by the European Union (project PI19/00449 to Dr. A. Lladó and project PI19/00198 to Dr M. Balasa), by Departament de Salut - Generalitat de Catalunya (PERIS 2016-2020 SLT008/18/00061 to Dr A. Lladó) and by Spanish Ministry of Science and Innovation (PID2020-118386RA-I00 to Dr. R. Sala-Llonch).